Experimental Evaluation of Frequency-dependent Conductivity using a Simultaneous Imaging of MREIT and MREPT

Munish Chauhan[1], Min Oh Kim[2], Woo Chul Jeong[1], Hyung Joong Kim[1], Oh In Kwon[3], Eung Je Woo[1], and Dong Hyun Kim[2]
[1]Kyung Hee University, Yongin, Gyeonggi, Korea, [2]Yonsei University, Seoul, Korea, [3]Konkuk University, Seoul, Korea

Target audience

This study might be helpful to the people who are interested in the electromagnetic tissue property mapping such as MREIT and MREPT.

Purpose

The purpose of this study is to understand the frequency-dependent conductivity through two different phantom imaging experiments using a simultaneous dual-frequency conductivity images.

Methods

For the simultaneous dual-frequency conductivity imaging experiment[1], we prepared an imaging object called the conductivity phantom whose conductivity distribution is predetermined and stable over time. A cylindrical acrylic phantom (12 cm diameter and 16 cm height) consisted of saline solution and two different diameter insulating films in a form of a hollow cylinder were used. One insulating film with 80 mm diameter was positioned at the center of phantom and the other film with 40 mm was located inside the bigger one (Fig. 1). To create a conductivity contrast, two different phantoms were designed to understand low- and high-frequency conductivity characteristics. In phantom A, each insulating films had equally-spaced 3 mm diameter of holes (8 holes in 80 mm, 4 holes in 40 mm) and filled both inside and outside of the hollow cylinder with the saline solution of 1.0 S/m conductivity. On the contrary, there were no holes on the insulating films of phantom B. But we filled inside of phantom with three different conductivities of saline solution with 2.0, 1.0, and 0.5 S/m, respectively (Fig. 1).

Four carbon-hydrogel electrodes were attached on the sides of the phantom and was placed the phantom inside the bore of 3T MRI scanner. Using a current source, the imaging currents (I_1 and I_2) were injected between one opposing pair of electrodes, respectively. The injection current amplitude was 3 mA with the total pulse width of 30 ms. The ICNE pulse sequence was used to obtain the MR magnitude and magnetic flux density (B_z) images.[2] The imaging parameters were as follows; TR/TE = 800/30 ms, FOV = 180×180 mm^2, slice thickness = 4 mm (8 slices), NEX = 8, matrix size = 128×128, and total imaging time = 40 min. For multi-slice conductivity image reconstructions, the B_z induced by externally injected currents and the B1+ phase map with injected current effects removed were acquired simultaneously. The low-frequency conductivity was reconstructed from the measured B_z by the single-step harmonic B_z algorithm while the high-frequency conductivity was reconstructed using the B1+ maps.[2]

Results and Discussion

Figure 2 shows typical results of simultaneous dual-frequency conductivity imaging in phantom A. The low-frequency conductivity image in Fig. 2b shows unique contrast inside the insulating film depending on the magnetic flux density by current flows.[3] Note that the high conductivity existing around the holes represents high current density due to the concentration of current flows. In the high-frequency conductivity image (Fig. 2c), however, there was no changes of conductivity contrast inside and outside of insulating film regardless of the presence or absence of holes.

Figure 3 shows results of phantom B. In case of insulating film without holes, the hollow cylindrical anomaly behaved as a solid insulator since the injected current at low frequency could not penetrate the thin insulating wall of the hollow cylinder (Fig. 3b). Therefore, the low-frequency conductivities inside the insulating films were quite lower than its actual values. On the other hand, the high-frequency conductivity image showed their conductivity values without being affected by the thin insulating films (Fig. 3c).

Conclusion

In this paper, we provide experimental evaluation of simultaneous dual-frequency conductivity imaging using a combination of MREIT and MREPT methods. These frequency-dependent conductivity spectra and values may provide new information on tissue structure and function, complementary to the information provided by traditional MRI.

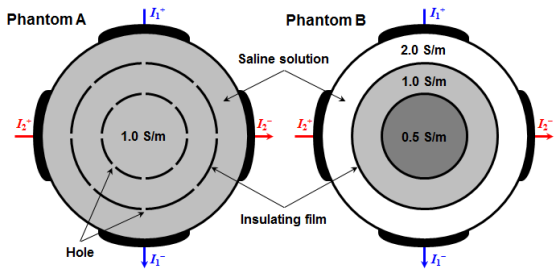

Fig. 1. Experimental setup for phantom imaging experiment. Two different phantoms were designed for the understanding of frequency-dependent conductivity.

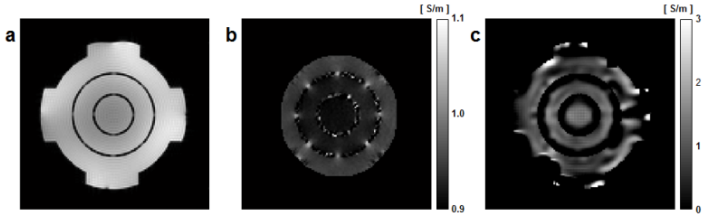

Fig. 2. (a) MR magnitude image shows the structural information of phantom A. (b) and (c) are reconstructed conductivity images at low- and high-frequency from MREIT and MREPT data, respectively.

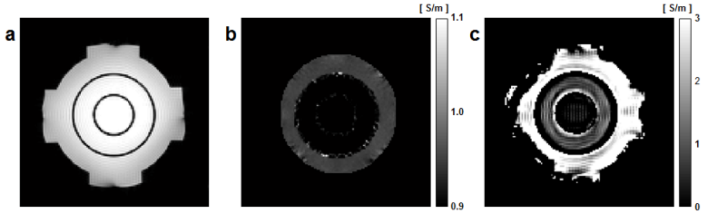

Fig. 3. (a) MR magnitude image shows the structural information of phantom B. (b) and (c) are reconstructed conductivity images at low- and high-frequency from MREIT and MREPT data, respectively.

References

1. Minhas AS, Kim YT, et al. Feasibility of dual-frequency conductivity imaging using MREIT and MREPT. In: Proceedings of the NFSI & ICBEM, Banff, Canada, 2011. p 68-71.
2. Seo JK, Kim M, et al. Error analysis of non-constant admittivity for MR-based electric property imaging. IEEE Trans Med Imaging 2012;31:430-437.
3. Oh TI, Kim YT, et al. Ion mobility imaging and contrast mechanism of apparent conductivity in MREIT. Phys Med Biol 2011; 56:2265-2277.